ATLAS NOTE

ATLAS-CONF-2011-158

November 18, 2011

Search for New Phenomena in Events with Three or more Charged Leptons

The ATLAS Collaboration

Abstract

We present a generic search for new phenomena in events with at least three charged leptons using 1.02 fb^{-1} of pp collision data recorded by the ATLAS detector at $\sqrt{s} = 7$ TeV. Events are selected with at least three isolated, charged leptons above 20 GeV with the leading lepton above 25 GeV and no identified $Z \rightarrow \ell^+\ell^-$ decays. After selection, 25.9 ± 3.8(stat) ± 4.3(syst) events are expected in the signal region from Standard Model backgrounds, and 31 events are observed. In a second signal region that uses a tighter lepton p_{T} cut at 30 GeV, 4.9 ± 1.6(stat) ± 0.9(syst) are expected from Standard Model sources, and 6 events are observed. The observed p-values for consistency with the Standard Model expectation are 27% and 33% in the two signal regions. Fiducial limits are extracted on models predicting excesses of multi-lepton events using pair production of doubly-charged Higgs bosons as a benchmark model. The observed fiducial cross-section limits are 38 fb and 14 fb in the two signal regions. Cross-section upper limits at the 95% confidence level are also set at 41 (34) pb for 200 (300) GeV excited electron neutrino pair production.

1 Introduction

A common signature of physics beyond the Standard Model (SM) is production of events with multiple charged leptons in the final state. Such events can be produced in models involving pair production of doubly-charged Higgs bosons [1, 2], supersymmetry [3, 4], extra gauge bosons (W' or Z') [5], seesaw mediators [6, 7], leptoquarks [8, 9], technicolor particles [10], heavy charged leptons [11] and excited neutrinos [12]. In this note, we present a generic search for events with three or more isolated charged leptons. Unless otherwise noted, leptons in this note refer to electrons or muons. No requirements are made on the number of jets nor on the missing transverse momentum ($E_{\mathrm{T}}^{\mathrm{miss}}$) in the event. The only event-level kinematic selection criterion for the signal region is the rejection of events with any opposite-sign (OS) same-flavor (SF) pair falling within 10 GeV of the Z mass. These leptonic Z decays are used as a control sample to estimate the expected background from continuum Drell-Yan and mismeasured Z boson events that also contain a third object misidentified as a lepton (a *fake* lepton). A second control sample consisting of $e\mu$ events with a third lepton candidate that fails the isolation requirement, is used to estimate the $t\bar{t}$ background. A third control sample of events with one isolated lepton and two non-isolated leptons is used to estimate the background from events with two fake leptons. The remaining backgrounds from dibosons and from $t\bar{t}$ produced in association with an extra W or Z boson, are estimated using Monte Carlo (MC) simulation. The SM expectation for the signal region is tested independently of any new physics (NP) model. Upper limits on the cross section for NP production of events with three or more charged leptons are set within a fiducial region using selection and reconstruction efficiencies for simulated pair production of doubly-charged Higgs bosons.

This analysis is complementary to but not independent of another search for evidence of NP in events with four or more charged leptons [13]. We also set limits on pair production of left-(right)-handed doubly-charged Higgs bosons. This analysis is complementary to a dedicated ATLAS doubly-charged Higgs search using same-sign dimuons [14], which rules out left-(right-)handed doubly-charged Higgs bosons at 95% confidence with masses less than 268(210) GeV. In addition, we set limits on pair production of excited electron neutrinos using a model with no electromagnetic coupling ($f = f'$, where f is the form factor associated with the SU(2) gauge group, and f' is the form factor associated with the U(1) gauge group). The H1 collaboration has ruled out single production of such objects with a mass less than 196 GeV [15]. More general pair production searches were made at LEP, and rule out excited neutrinos for $f = f'$ with masses less than 101 GeV [16, 17]. CMS has also searched for evidence of NP in events with three or more charged leptons in 2.1fb-1 of data [18]. Their results are mostly consistent with Standard Model expectations.

2 Detector, data and Monte Carlo simulation

The ATLAS detector [19] is a multi-purpose high-energy physics experiment observing pp collisions at the LHC. The inner detector (ID) system of the ATLAS detector is immersed in a superconducting solenoid providing a 2 T magnetic field, and provides precision tracking of charged particles. The ID consists of a silicon pixel detector and silicon strip detector covering pseudorapidity $|\eta| < 2.5$, and a straw-tube tracker covering $|\eta| < 2$, where $\eta = -\ln\tan(\frac{\theta}{2})$ and θ is the polar angle with respect to the LHC beamline. Outside of the solenoid are electromagetic and hadronic calorimeters covering the range $|\eta| < 4.9$. The outermost part of the ATLAS detector is a muon spectrometer (MS) with a toroidal magnetic field, providing separate trigger and precision tracking chambers for muons with $|\eta| < 2.4$ and $|\eta| < 2.7$, respectively.

A multi-level trigger system selects events for offline analysis. The events in this analysis were selected using single-lepton triggers with thresholds of 20 GeV of transverse energy (E_{T}) for electrons and 18 GeV of transverse momentum (p_{T}) for muons. The efficiencies of the single-lepton triggers have been determined as a function of lepton p_{T} or E_{T} using large samples of $Z \rightarrow \ell\ell$ events. The trigger efficiency for events with three or more charged leptons is very close to 100%.

The analysis in this note uses a data sample of proton-proton collisions at $\sqrt{s} = 7$ TeV recorded between March and June 2011. Data periods flagged with data quality problems are removed. After data quality cuts, the total integrated luminosity used in the analysis is 1.02 fb^{-1}, with an uncertainty of 3.7% [20].

Several samples of Monte Carlo events are used to estimate backgrounds and understand control regions. Detector response is simulated [21] with a program based on GEANT4 [22]. ALPGEN [23] and PYTHIA [24] are used to study Z+jets backgrounds, which are normalized to next-to-next-to-leading-order (NNLO) predictions. Samples of $t\bar{t}$ and single-top production are generated using MC@NLO [25] and are normalized to NNLO predictions. Diboson samples are generated using HERWIG [26], with cross sections normalized to next-to-leading-order (NLO) predictions. Production of $t\bar{t}$ pairs with additional vector bosons is generated using MADGRAPH [27], with showering and hadronization performed by PYTHIA. The doubly-charged Higgs boson signal is also generated using MADGRAPH and PYTHIA. The doubly-charged Higgs bosons are allowed to decay democratically with equal branching fraction to any combination of same-sign charged leptons, including τ leptons. The cross section depends on whether the doubly-charged Higgs is produced in a right-handed or left-handed model, and is normalized to NLO predictions. The excited electron neutrino signal is generated with COMPHEP [28, 29] and PYTHIA. The excited electron neutrinos can decay to either a neutrino and a Z boson or an electron and a W boson. All Monte Carlo simulations are reweighted to reproduce the distribution of the number of inelastic pp collisions per bunch-crossing observed in the data.

3 Event selection

Signal events must contain at least three high-p_{T} isolated electrons or muons. To ensure that they originate from the primary vertex, each lepton candidate is required to have a longitudinal impact parameter (distance of closest approach) with respect to the primary vertex of less than 10 mm and a transverse impact parameter significance (transverse impact parameter divided by its error) of less than 10.

Muons are identified by matching tracks reconstructed in the MS to tracks reconstructed in the ID. Only muons with $p_{\mathrm{T}} > 20$ GeV and $|\eta| < 2.5$ are considered. In order to reject non-isolated muons from sources such as the decay of heavy-flavor quarks, pions and kaons, the scalar sum of transverse momenta (Σp_{T}) of all other tracks inside a cone of $\Delta R \equiv \sqrt{(\Delta\eta)^2 + (\Delta\phi)^2} = 0.2$ around the muon must be less than 10% of the muon p_{T}. Tracks entering the sum are required to have at least four hits in the silicon detectors and $p_{\mathrm{T}} > 1$ GeV.

Electrons are reconstructed from a cluster in the electromagnetic calorimeter matched to a track in the ID. Candidates are required to have a transverse energy as measured in the calorimeter of at least 20 GeV, and a pseudorapidity $|\eta| < 2.47$. Electrons in the barrel–endcap transition region at $1.37 < |\eta| < 1.52$ are rejected. The standard ATLAS "tight" electron selection is used [30]. Electrons are also required to be isolated from other activity: the transverse energy measured in the calorimeter inside a cone of $\Delta R = 0.2$ around the electron but excluding the electron E_{T} is required to be less than 10% of the electron E_{T}. The energy in this cone is corrected for pile-up effects due to additional pp interactions in the bunch crossing.

Electron candidates within $\Delta R = 0.1$ of any selected muon are rejected, and if two electron candidates are within $\Delta R = 0.1$ of each other, the one with the lower E_{T} is rejected. In order to remove non-collision backgrounds, events are required to contain at least one vertex formed from at least three good tracks [31] with $p_{\mathrm{T}} > 0.5$ GeV. The vertex with the largest sum of the p_{T}^2 computed with the associated tracks is selected as the primary vertex.

Scale factors are applied to the simulation to correct for differences in lepton reconstruction and identification between simulation and data. These scale factors have values that vary from unity by

1–3% for both muons [32] and electrons [30] depending on the p_{T} (for muons) or E_{T} (for electrons).

The $E_{\mathrm{T}}^{\mathrm{miss}}$ in the event is calculated as the negative vector sum of the transverse components of energy deposits in the calorimeters within $|\eta| < 4.5$. For events containing muons, any calorimeter energy deposit from a muon is ignored and the muon energy measured in the MS is used instead.

Events are required to have at least three leptons selected as above, and to have passed the single-muon or single-electron triggers mentioned earlier. To ensure a well-measured trigger efficiency, at least one of these muons (electrons) must have $p_{\mathrm{T}}(E_{\mathrm{T}}) > 25$ GeV. We reject events with any OS-SF pair with a dilepton mass less than 20 GeV. Events with a candidate Z boson are also rejected: if there is an OS-SF pair with a dilepton mass within 10 GeV of the Z mass, the event is rejected from the signal region, and is instead used in a control region to estimate fakes. The above selection defines the nominal signal region. A second, tighter signal region requiring the $p_{\mathrm{T}}(E_{\mathrm{T}})$ of all three leptons to be above 30 GeV is also defined. This second signal region has a significantly reduced number of events with fake leptons, yet still maintains high efficiency for many NP models.

4 Background estimation

The only significant SM sources of events with at least three real isolated leptons are diboson production ($pp \to WZ$ or ZZ), and the production of $t\bar{t}$ pairs in association with extra vector bosons. Aside from these events, which are estimated from Monte Carlo simulation, the signal region for this search is dominated by events with one or two real isolated leptons from either dilepton $t\bar{t}$, Z/γ^{*}, or W bosons, plus one or more leptons not from a W or Z decay (a fake). In this note, sources of fakes include true leptons from heavy-flavor jets, photon conversions, and muons from in-flight decays of kaons and pions. As described below, the fake background is estimated using techniques designed to make maximal use of the data itself while having minimal reliance on Monte Carlo simulation. We determine the fake backgrounds from $t\bar{t}$, Z+jets and W+jets separately. The rationale behind this is that fakes from $t\bar{t}$ are dominantly from the b-jets in top dilepton events, while fakes from the W/Z+jets backgrounds are a mix of heavy-flavor and gluon/light-flavor jets; additionally, these three sources can be checked independently in different control regions. Trilepton events from $W\gamma^{*}$ production are estimated to be negligible. Small additional backgrounds that are estimated from simulation include $Z \to \tau\tau$+jets and single top production. Dalitz decays of the Z boson with an internal photon in the matrix element that decays to a dilepton pair represent another potential source of Z bosons in the signal region. Monte Carlo simulation shows that this process should be negligible. Several event selection criteria reduce this background, including the minimum $p_{\mathrm{T}}(E_{\mathrm{T}})$ requirements, isolation requirements, and the requirement that there be no OS-SF pair with dilepton mass below 20 GeV.

4.1 QCD multijet templates

The fake lepton background estimates in the following sections rely on knowing the isolation distribution of fake leptons. These distributions are obtained from QCD multijet data by removing the isolation requirement on lepton candidates and then vetoing events consistent with coming from processes that produce real leptons. Events with a single lepton are required to have a transverse mass (computed from the charged lepton and the $E_{\mathrm{T}}^{\mathrm{miss}}$) less than 40 GeV, and events with two leptons must not have an OS-SF pair within ± 25 GeV around the Z mass. The small remaining real lepton contamination on the order of a few percent is subtracted using MC simulation. The data are then binned in the number of jets and fake lepton p_{T}. To study systematic uncertainties on these distributions arising from variations in the heavy-flavor fraction, electron fakes are also obtained from categories enriched and reduced in heavy-flavor by dividing into two categories depending on whether electrons pass or fail a cut on the amount of transition radiation detected in the straw-tube tracker.

4.2 Z+jets estimation

The background in the signal region from Z+jets with an additional fake lepton is estimated using data events. First, a control sample of trilepton events consistent with the production of Z bosons is selected by requiring OS-SF leptons with a dilepton mass within 10 GeV of the Z mass. All selection criteria described in Section 3 except for the Z mass veto are applied. This control sample is expected to be dominated by diboson events with a Z boson (WZ/ZZ). Monte Carlo studies indicate that Z+jets events with an additional fake lepton contribute approximately 10% of the sample.

Two additional criteria are then added to enhance the fraction of events with a fake lepton. The first is a very loose requirement of $E_{\mathrm{T}}^{\mathrm{miss}} < 50$ GeV (an anti-$E_{\mathrm{T}}^{\mathrm{miss}}$cut). This reduces the WZ contribution by almost a factor of two while removing only a few percent of the Z+jets fakes. Thus, it does not significantly alter the heavy-flavor fraction of the fake leptons. In a second requirement, the relative isolation cut is relaxed from 0.1 to 0.5. This significantly increases the number of Z+jets events, allowing for a higher statistics extrapolation into the signal region.

To calculate the background in the signal sample, the Z control sample must be corrected for the predicted number of events from sources other than Z+jets. This gives the number of Z+jets events with the looser isolation and anti-$E_{\mathrm{T}}^{\mathrm{miss}}$ cut. Monte Carlo simulation is then used to scale from the number of Z+jets trilepton events with the loose anti-$E_{\mathrm{T}}^{\mathrm{miss}}$ selection criteria to the number with no $E_{\mathrm{T}}^{\mathrm{miss}}$ requirement. Finally, the isolation distribution for fake leptons obtained from multijet data is used to scale the number of events found in data that pass the loose isolation criteria to the signal region defined by the tight isolation criteria. This scaling is summarized in Equation 1:

$$\begin{aligned} N^{SR}_{Z,Est.} &= R_{iso} \cdot R_{MET} \cdot R_{m_{ll}} \cdot (N^{CR-Z}_{Obs.,Data} - N^{CR-Z}_{BG,MC}) \\ R_{MET} &= \frac{N^{SR}_{Z,MC}}{N^{SR,MET}_{Z,MC}} \\ R_{m_{ll}} &= \frac{N^{SR}_{Z,MC}}{N^{SR,m_{ll}}_{Z,MC}} \end{aligned} \tag{1}$$

where $N^{SR}_{Z,Est.}$ is the estimated Z+jets yield in the signal region, $N^{CR-Z}_{Obs.,Data}$ is the observed data in the Z control region with the anti-$E_{\mathrm{T}}^{\mathrm{miss}}$ cut and loosened isolation, and $N^{CR-Z}_{BG,MC}$ is the expected number of events in that control region, not including Z+fake events. $N^{SR}_{Z,MC}$ is the signal region estimated yield from simulation; $N^{SR,MET}_{Z,MC}$ is the expected Z+fake yield, from simulation, in the signal region with an anti-$E_{\mathrm{T}}^{\mathrm{miss}}$ cut, and $N^{SR,m_{ll}}_{Z,MC}$ is the expected Z+fake yield with an OS-SF mass within 10 GeV of the Z mass, given by Monte Carlo simulation. The three R terms scale the yields from the control region to the signal region. The R_{MET} and $R_{m_{ll}}$ terms come from Monte Carlo simulation, and scale from the dilepton Z mass region with an anti-$E_{\mathrm{T}}^{\mathrm{miss}}$ cut to the signal region. As mentioned above, the anti-$E_{\mathrm{T}}^{\mathrm{miss}}$ cut has almost no effect, so that R_{MET} is nearly 1.0. The R_{iso} term comes from QCD multijet data, and is an efficiency for fake leptons to pass the nominal isolation cut, given that they have passed the loose isolation selection criteria. These three terms are derived separately for events with a fake electron and events with a fake muon. The expected and observed events counts are summarized in Table 1. The p_{T} of the third lepton in events inside the Z control region after the anti-$E_{\mathrm{T}}^{\mathrm{miss}}$ requirement and the less restrictive isolation requirement are shown in Figure 1. The Monte Carlo simulation reproduces the overall fake rate within the large statistical uncertainty, although the average p_{T} of fakes in data may be lower than in the simulation. With the tighter lepton selection, the method is statistically limited by the data and predicts $1.0^{+1.5}_{-1.0}$ events in the signal region.

Table 1: Table of the yields and expectations in the Z+jets control and signal regions for the nominal signal region. The quoted uncertainty is the statistical uncertainty on the data.

	Z+fake electron	Z+fake muon
$N^{SR}_{Z,MC}$	5.8	1.9
$N^{CR-Z}_{BG,MC}$	27.7	32.2
$N^{CR-Z}_{Obs.,Data}$	43	59
$N^{SR,MET}_{Z,MC}$	5.8	1.9
$N^{SR,m_{ll}}_{Z,MC}$	8.4	5.5
R_{iso}	0.53	0.24
$N^{SR}_{Z,Est.}$	5.6±3.1	2.3±0.8

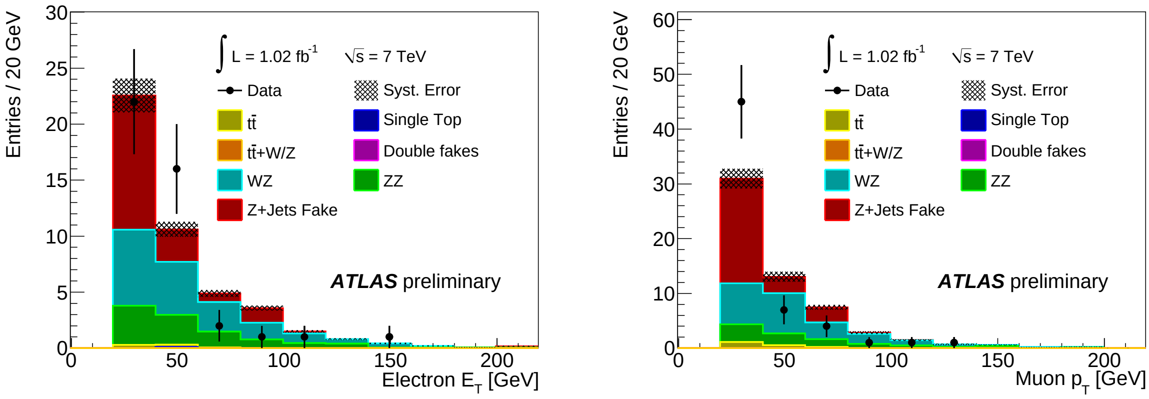

(a) (b)

Figure 1: Non-Z electron E_T (a) and muon p_T (b) after the anti-E_T^{miss} requirement and the loosening of the isolation. The shape and magnitude of the Z+jets background is taken directly from simulation, and is not scaled to the data-driven estimate.

4.3 $t\bar{t}$ estimation

The contribution from $t\bar{t}$ to the signal sample is estimated using a control sample enriched in $t\bar{t}$ events and an additional fake lepton. Events containing one electron and one muon passing all lepton selection criteria, plus an additional third lepton that fails only the isolation requirement and has a $p_T > 15$ GeV (instead of the nominal 20 GeV requirement), are selected. To reduce Z boson contamination, events are required to have E_T^{miss} in excess of 20 GeV. The expected non-top contributions to this sample from SM sources are expected to be small and are estimated from Monte Carlo simulation.

The $t\bar{t}$ estimate is determined using the following expression:

$$N^{SR}_{t\bar{t},Est.} = R_{t\bar{t},MC} \cdot (N^{CR}_{Obs.,Data} - N^{CR}_{BG,MC})$$
$$\text{with} \quad R_{t\bar{t},MC} = \frac{N^{SR}_{t\bar{t},MC}}{N^{CR}_{t\bar{t},MC}} \tag{2}$$

where $N^{SR}_{t\bar{t},Est.}$ is the estimated $t\bar{t}$ yield in the signal region, $N^{SR(CR)}_{t\bar{t},MC}$ is the expected event yield in the signal (control) region as measured in $t\bar{t}$ MC simulation and $N^{CR}_{Obs.,Data(BG,MC)}$ is the observed (expected from simulation) yield of (non-$t\bar{t}$ background) events in the control region. Scale factors that account for

Table 2: Table of the yields and expectation in the $t\bar{t}$ signal and control regions. Systematic uncertainties are shown for MC yields and statistical uncertainties are shown for data. The final estimate has both statistical and systematic uncertainties.

	Nominal signal selection		Tighter selection	
Variable	Electrons	Muons	Electrons	Muons
$N^{SR}_{t\bar{t},MC}$	2.3 ± 0.3	3.8 ± 0.3	0.7 ± 0.1	0.7 ± 0.1
$N^{CR}_{t\bar{t},MC}$	4.0 ± 0.5	54.8 ± 3.2	4.0 ± 0.5	54.8 ± 3.2
$N^{CR}_{Obs.,Data}$	8	76	8	76
$N^{CR}_{BG,MC}$	1.2 ± 0.3	7.4 ± 1.3	1.2 ± 0.3	7.4 ± 1.3
$N^{SR}_{t\bar{t},Est.}$	3.9 ± 1.6(stat) ± 0.5(syst)	4.8 ± 0.6(stat) ± 0.2(syst)	1.1 ± 0.5(stat) ± 0.2(syst)	0.9 ± 0.1(stat) ± 0.1(syst)

data-MC differences in the isolation efficiency are estimated using heavy-flavor-enriched QCD multijet data. This procedure is performed separately for the two sets of signal selection criteria and two lepton flavors.

Table 2 shows the measured values in Equation 2 as well as the $t\bar{t}$ background estimate for both signal samples. There are significantly more muons than electrons in the control region. This is because the tight electron identification includes other shower shape and calorimeter-based cuts that reject fakes, whereas muons rely predominantly on isolation to reject fakes. Figure 2 shows kinematics distributions for events that pass the $t\bar{t}$ control region selection criteria. The $E_{\mathrm{T}}^{\mathrm{miss}}$ cut is effective at removing Z boson contamination, after which it can be seen that the MC simulation slightly underestimates the heavy-flavor fake rate.

4.4 Double fakes

The background in the signal region from events with two fakes is measured in data by scaling the yield in a control region dominated by two fakes. This control region is defined by events with exactly one lepton that passes all of the lepton selection criteria and exactly two leptons that pass all those requirements but fail the isolation requirement. A small contamination from Z bosons plus one fake is removed by vetoing events with an OS-SF lepton pair within 10 GeV of the Z mass. The scaling factor to the isolated signal region is then given by $\frac{\epsilon}{1-\epsilon}$, where ϵ is the efficiency for QCD multijet events to pass the isolation cut given that they passed all other lepton selection criteria. This efficiency is determined from QCD multijet data templates, and is binned in lepton p_{T} and the number of jets. The predicted double fake background in the nominal signal region is 5.1 ± 1.1(stat) $^{+1.7}_{-1.4}$(syst), and 0.2 ± 0.2(stat) ± 0.0(syst) in the tighter signal region. The double fakes are dominated by events with leptonically decaying W bosons plus two fakes from jets, but include other types of events.

5 Systematic uncertainties

A wide range of potential systematic uncertainties are evaluated for all background estimates and event yields predicted by NP models. The dominant source of systematic uncertainty on the estimates for both $t\bar{t}$ and Z+jets backgrounds is the ability to scale from one lepton isolation range to another using QCD multijet events. These isolation efficiencies vary with fake lepton p_{T} and the number of jets. The $t\bar{t}$ and Z+jets fake measurements are repeated using isolation efficiencies from different lepton p_{T} ranges and jet multiplicities, leading to uncertainties of 23–25%. In addition, the $t\bar{t}$ and Z+jets measurements scale from control regions to one of the two signal regions, which require accurate Monte Carlo simulation in the signal region. The Z+fake measurements are partially limited by MC statistics, leading to a

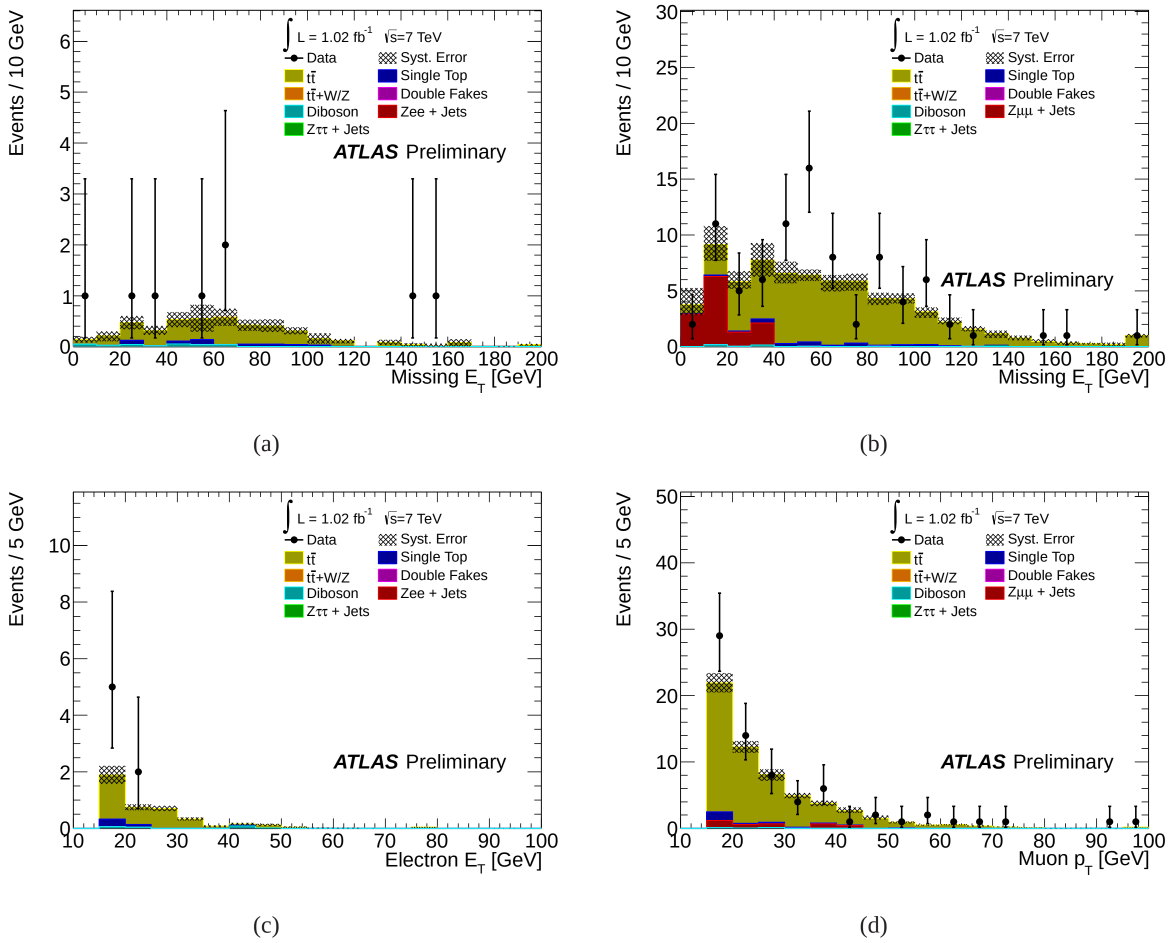

Figure 2: Kinematic distributions in the $t\bar{t}$ control region. The $E_{\mathrm{T}}^{\mathrm{miss}}$ is shown on the top, and the E_{T} (p_{T}) of the non-isolated electron (muon) is shown on the bottom after requiring $E_{\mathrm{T}}^{\mathrm{miss}} > 20$ GeV. Plots are made without any scaling of Monte Carlo expectation to the data-based estimates. Plots on the left (right) have non-isolated electrons (muons) as the third lepton. Uncertainties on data are given by Poisson statistics.

14.6% (25.0%) systematic uncertainty on the Z+fake electron (muon) measurement. The uncertainties due to limited MC statistics for the $t\bar{t}$ fake estimates are 7.6 (4.8)% in the electron (muon) channels. The 25–33% systematic uncertainty on the double fake measurement is dominated by uncertainties obtained when varying the heavy-flavor fraction of the fake templates. A variety of other smaller systematics are also evaluated for all background estimates, including luminosity uncertainties, cross-section uncertainties and uncertainties on lepton identification and trigger scale factors.

6 Results

Table 3 summarizes the estimated backgrounds for each source in both signal regions. A total of 25.9 ± 3.8(stat) ± 4.3(syst) events are predicted from SM sources in the nominal signal region. In the full dataset, 31 events are observed. In the second, restrictive signal region, 4.9 ± 1.6(stat) ± 0.9(syst) are expected from SM sources, and 6 events are observed. Figures 3 and 4 show distributions of kinematic variables for the data in the nominal signal region. No significant excesses are seen at high values of $E_{\mathrm{T}}^{\mathrm{miss}}$ or lepton p_{T}.

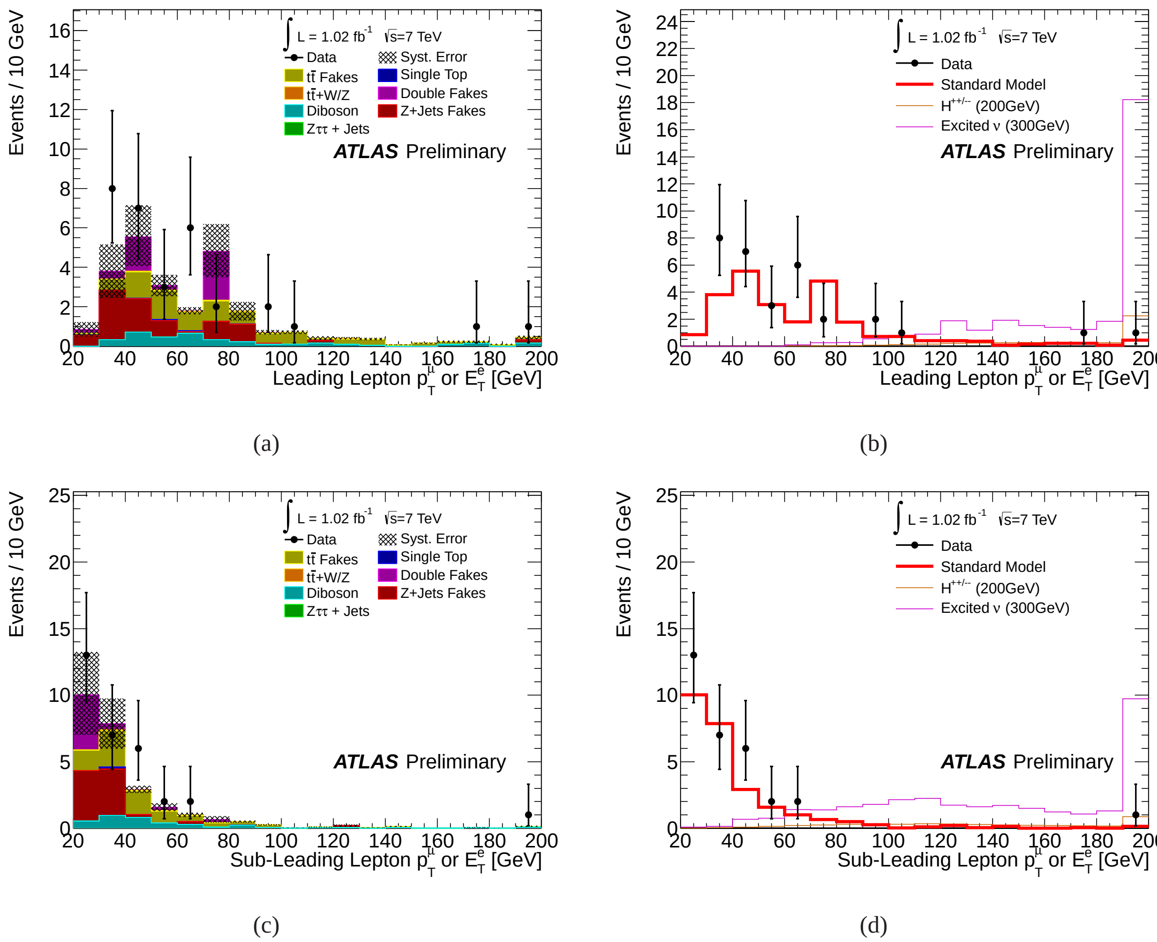

Figure 3: Leading lepton $E_{\mathrm{T}}(p_{\mathrm{T}})$ (a-b) and subleading lepton $E_{\mathrm{T}}(p_{\mathrm{T}})$ (c-d) in trilepton events with SM expectations stacked (a,c) and with models of NP overlaid (b,d) for both electrons and muons. Standard Model refers to the sum of all expectations from Standard Model processes, including those with fake leptons. The last bin in all plots is an overflow bin.

7 Limits

The MCLIMIT [33, 34] software package is used to calculate an expected and observed CL_S given the observed event yield, the predicted signal event yield, the predicted background yield and the systematic uncertainties (including correlations between signal and background). The profile likelihood technique is used to incorporate systematic uncertainties. The observed p-values for consistency with the SM

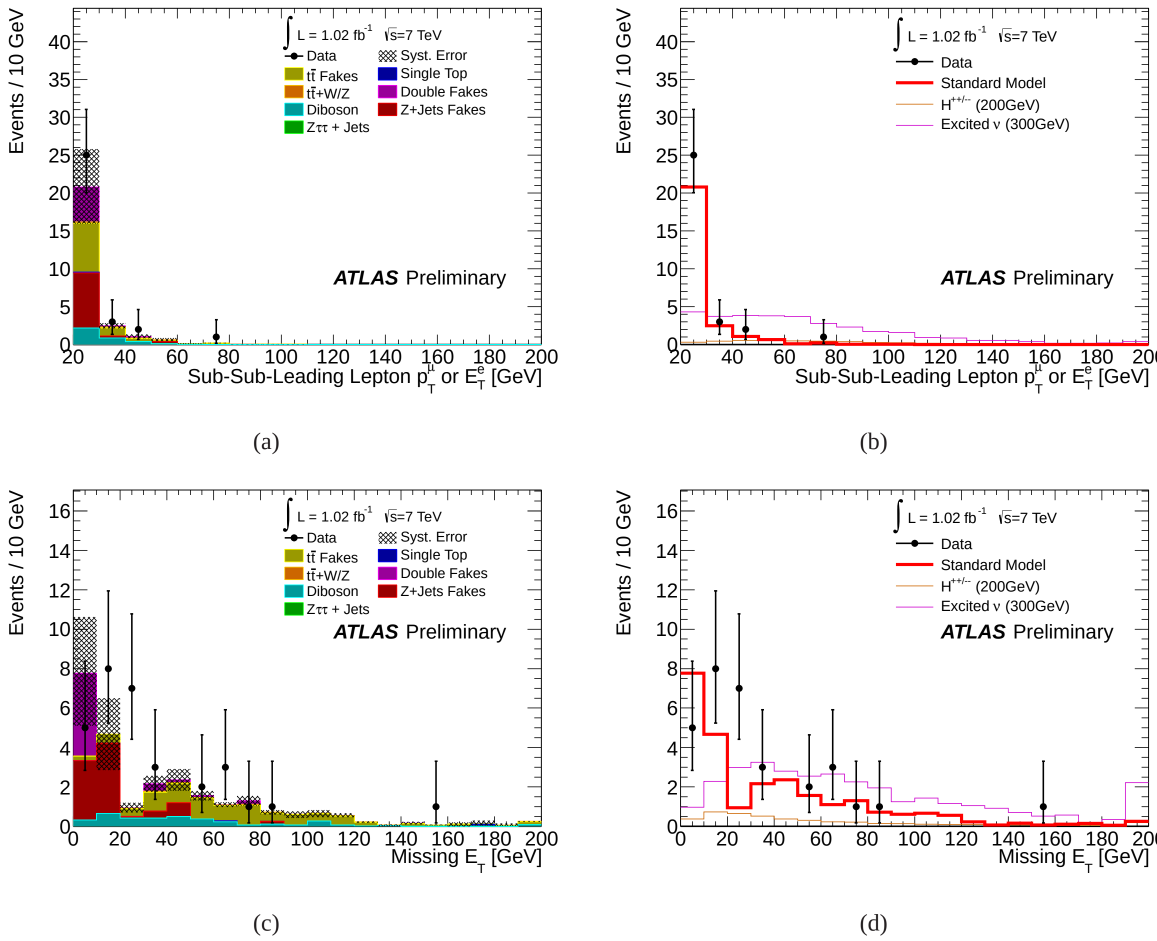

Figure 4: Sub-sub-leading lepton $E_{\mathrm{T}}(p_{\mathrm{T}})$ (a-b) for both electrons and muons and $E_{\mathrm{T}}^{\mathrm{miss}}$ (c-d) in trilepton events with SM stacked (a,c) and with models of NP overlaid (b,d). Standard Model refers to the sum of all expectations from Standard Model processes, including those with fake leptons. The last bin in all plots is an overflow bin.

expectations are 27% and 33% in the two signal regions. In the absence of evidence for NP, the yields are interpreted as an exclusion on a number of NP scenarios. Using a MC simulation of pair-produced doubly-charged Higgs bosons as a generic model, an upper limit is extracted on the maximum expected yield of events from NP in the data sample. The doubly-charged Higgs bosons model decays with equal branching fraction to all lepton flavors and thus is more generic than the exited electron neutrino model.

To make limits on NP models generic, we define fiducial regions at the parton level. For the nominal signal selection, the fiducial region contains events with three or more charged leptons (e or μ) each with $p_{\mathrm{T}} > 20$ GeV and $|\eta| < 2.5$ with no opposite-sign same-flavor pair whose invariant mass, m_{ll}, falls into the window [81,101] GeV. With the tighter signal region, the fiducial region has the p_{T} threshold raised to 30 GeV. Within these regions, the trilepton selection efficiency is calculated for several NP models. Table 4 shows, for these models, the fraction of events falling in or out of the fiducial region and the selection efficiency for each region. The LH and RH doubly charged Higgs models use the same MC samples, and differ only in the production cross sections. Using the lowest doubly-charged Higgs boson selection efficiency for each fiducial region, fiducial limits are extracted for models predicting excesses of multi-lepton events. As shown in Table 5, the observed 95% confidence level upper limits on fiducial

Table 3: The estimated Standard Model background and NP yields in the nominal and tighter signal regions, together with the observed event counts in data. Where two uncertainties are given, the first is from data statistics, and the second is from systematic uncertainties.

Process	Yield (nominal signal selection)	Yield (tighter signal selection)
Z+jets	7.9 ± 3.2± 2.4	1.0 ± 1.5
$t\bar{t} + e$ Fake	3.9 ± 1.6± 0.5	1.1 ± 0.5± 0.2
$t\bar{t} + \mu$ Fake	4.8 ± 0.6± 0.2	0.9 ± 0.1± 0.1
Z$\rightarrow \tau\tau$+jets	0 ± 0.6	0 ± 0.6
Double Fakes	$5.1 \pm 1.1^{+1.7}_{-1.4}$	0.2 ± 0.2± 0.0
Diboson	3.6 ± 0.4	1.5 ± 0.2
Single Top	0.1 ± 0.1	0.0 ± 0.0
$t\bar{t}$+W/Z	0.5 ± 0.0	0.3 ± 0.0
Total Background	25.9 ± 3.8± 4.3	4.9 ± 1.6± 0.9
H$^{++/--}$ (LH m_H=200 GeV)	4.5 ± 0.2	4.2 ± 0.2
Data	31	6

Table 4: Fiducial fraction and selection efficiency for two NP models. Events can either fall inside or outside of the fiducial region; the fraction of events falling into each category is shown. For the two regions, events can pass or fail the full selection criteria. These efficiencies are also shown. As expected, the efficiency to pass full selection criteria is close to zero for events outside of the fiducial region.

	Outside fiducial region		Inside fiducial region	
Source	Fraction	Selection efficiency	Fraction	Selection efficiency
Nominal signal region				
H$^{++/--}$ (100 GeV)	0.57	0.02	0.43	0.57
H$^{++/--}$ (150 GeV)	0.46	0.03	0.54	0.61
H$^{++/--}$ (200 GeV)	0.39	0.03	0.61	0.63
H$^{++/--}$ (300 GeV)	0.33	0.03	0.67	0.65
Excited ν (200 GeV)	0.51	0.02	0.49	0.47
Excited ν (300 GeV)	0.48	0.03	0.52	0.52
Tighter signal region				
H$^{++/--}$ (100 GeV)	0.68	0.02	0.32	0.57
H$^{++/--}$ (150 GeV)	0.53	0.02	0.47	0.61
H$^{++/--}$ (200 GeV)	0.44	0.03	0.56	0.63
H$^{++/--}$ (300 GeV)	0.36	0.03	0.64	0.66
Excited ν (200 GeV)	0.61	0.02	0.39	0.49
Excited ν (300 GeV)	0.55	0.02	0.45	0.52

cross sections are 38 fb and 14 fb in the two signal regions, with expected limits of 28 fb and 11 fb. As no isolation requirement is made at the parton level, these limits may be slightly worse for models with significant additional jet activity. Figure 5 shows the expected and observed cross-section upper limits (at 95% confidence level) on $H^{++}H^{--}$ production as a function of the mass of the doubly-charged Higgs boson. Cross-section upper limits at a 95% confidence level are also set at 41 (34) fb for 200 (300) GeV excited electron neutrino pair production, improving on the limits set at LEP.

Table 5: Expected and observed fiducial cross-section limits.

	Expected fiducial limits (fb)	Observed fiducial limits (fb)
Nominal signal region	28	38
Tighter signal region	11	14

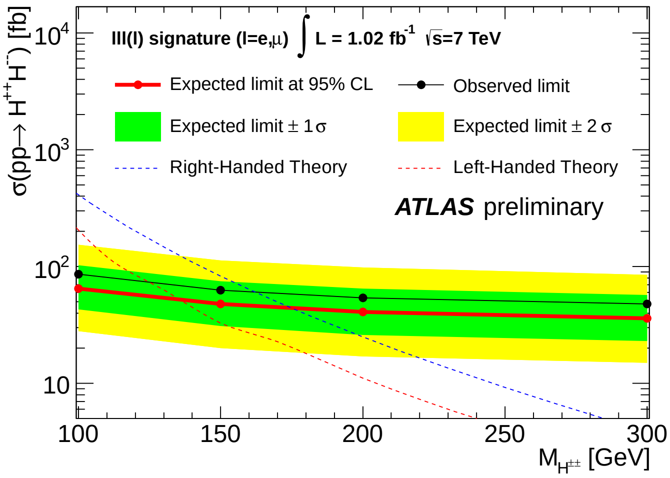

(a)

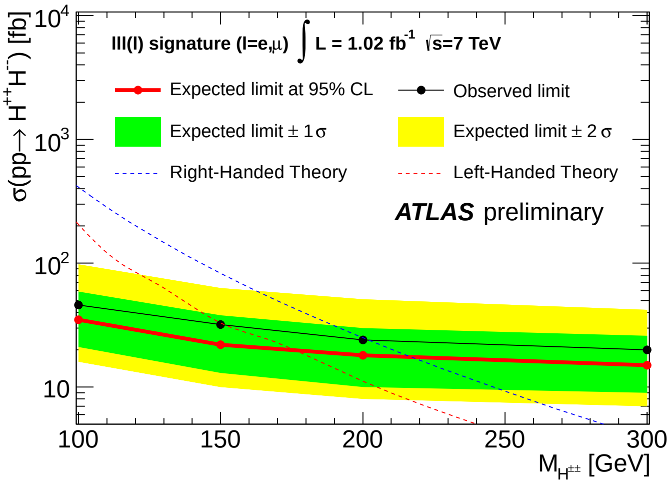

(b)

Figure 5: Expected and observed cross-section limits on the $H^{++}H^{--}$ model as a function of the doubly-charged Higgs mass. The expected limit is shown in red with uncertainty bands for $\pm 1\ \sigma$ (green) and $\pm 2\ \sigma$ (yellow). The limits are shown for the nominal signal region (a) and the tighter signal region (b).

8 Conclusions

A generic search for an excess of events with three or more charged leptons inconsistent with Z boson production was made. No requirements on observed jet activity or missing transverse energy were included. Using 1.02 fb^{-1} of data, 31 events with three leptons were observed with a SM expectation of

$25.9 \pm 3.8(\text{stat}) \pm 4.3(\text{syst})$. Using a tighter lepton p_{T} selection, $4.9 \pm 1.6(\text{stat}) \pm 0.9(\text{syst})$ were expected, and 6 events were observed. No significant excesses were seen at high values of $E_{\mathrm{T}}^{\mathrm{miss}}$ or lepton p_{T}. The observed p-values for consistency with the SM expectations are 27% and 33% in the two regions. The observed fiducial cross-section limits are 38 fb and 14 fb in the two regions. Cross-section upper limits at a 95% confidence level are also set at 41 (34) pb for 200 (300) GeV excited electron neutrino production, improving on the limits set at LEP on excited neutrino pair production.

References

[1] T. Rizzo, *Doubly charged Higgs bosons and lepton-number-violating processes*, Phys. Rev. **D 25** (1982) 1355; addendum ibid **27** (1983) 657.

[2] V. Rentala, W. Shepherd and S. Su, *A Simplified Model Approach to Same-sign Dilepton Resonances*, Phys. Rev. **D 85** (2011) 35004.

[3] V. Barger and H.-S. Lee, *Four-lepton Resonance at the Large Hadron Collider*, arXiv:hep-ph/1111.0633v2 (2011) .

[4] G. S. V. Barger and B. Yencho, *Many Leptons at the LHC from the NMSSM*, arXiv:hep-ph/1011.3526 (2011) .

[5] P. Langacker, *The physics of heavy Z' gauge bosons*, Rev. Mod. Phys. **81** (2009) 1199.

[6] F. del Aguila and J. Aguilar-Saavedra, *Distinguishing seesaw models at LHC with multi-lepton signals*, Nucl. Phys. B **813** (2009) 22.

[7] S. Matsumoto, T. Nabeshimaa, K. Yoshiokab, *Seesaw Neutrino Signals at the Large Hadron Collider*, JHEP **06** (2010) 058, arXiv:1004.3852.

[8] H. Harari, *A schematic model of quarks and leptons*, Phys. Lett. **B 86** (1979) 83.

[9] B. Schrempp and F. Schrempp, *Light leptoquarks*, Phys. Lett. **B 153** (1985) 101.

[10] E. Eichten and K. Lane, *Dynamical breaking of weak interaction symmetries*, Phys. Lett. **B 90** (1980) 125.

[11] V. E. Ozcan, S. Sultansoy and G. Unel, *Possible Discovery Channel for New Charged Leptons at the LHC*, J. Phys. G: Nucl. Part. Phys. **37** (2010) 059801.

[12] A. Belyaev, C. Leroy and R. Mehdiyev, *Production of Excited Neutrino at the LHC*, Eur. Phys. J. **C 41** (2005) 1–10.

[13] ATLAS Collaboration, *Search for New Phenomena in Events with Four Charged Leptons*, ATLAS-CONF-2011-144.

[14] ATLAS Collaboration, *Search for Doubly Charged Higgs Boson Production in Like-sign Muon Pairs in pp Collisions at $\sqrt{s}$=7 TeV*, ATLAS-CONF-2011-127 .

[15] H1 Collaboration, F.D. Aaron et al., *A search for excited neutrinos in ep collisions at HERA*, Phys. Lett. B. **663** (2008) 382–389.

[16] P. Achard et al., *Search for Excited Leptons at LEP*, Phys. Lett. B **568** (2003) 23.

[17] DELPHI Collaboration, J. Abdallah et al., *Search for excited leptons in e+e collisions at $\sqrt{s}$ = 189-209 GeV*, Eur. Phys. J. C **46** (2006) 277.

[18] CMS Collaboration, *Searches for Supersymmetry using Multilepton Signatures in pp Collisions at 7 TeV, CMS PAS SUS-11-013*, http://cdsweb.cern.ch/record/1393719/files/SUS-11-013-pas.pdf.

[19] ATLAS Collaboration, *The ATLAS Experiment at the CERN Large Hadron Collider*, JINST **3** (2008) S08003.

[20] ATLAS Collaboration, *Luminosity Determination in pp Collisions at* $\sqrt{s} = 7$ TeV *using the ATLAS Detector in 2011*, ATLAS-CONF-2011-116.

[21] ATLAS Collaboration, *The ATLAS Simulation Infrastructure*, Eur. Phys. J. **C 70** (2010) 823.

[22] S. Agostinelli et al., *Geant4 – a simulation Toolkit*, Nucl. Instrum. Meth. **A 506** (2003) 250.

[23] M. L. Mangano, M. Moretti, F. Piccinini, R. Pittau, and A. Polosa, *ALPGEN, a generator for hard multiparton processes in hadronic collisions*, JHEP **0307** (2003) .

[24] T. Sjostrand et al., *High-energy physics event generation with PYTHIA 6.1*, Comput. Phys. Commun. **135** (2001) 238–259.

[25] S. Frixione and B.R. Webber, *Matching NLO QCD Computations and parton shower simulations*, J. High Energy Phys. **0206** (2002) 029.

[26] G. Corcella, I. Knowles, G. Marchesini, S. Moretti, K. Odagiri, P. Richardson, M. Seymour, and W. B, *HERWIG 6.5*, JHEP **0101** (2001) 010.

[27] J. Alwall et al., *MadGraph/MadEvent v4: The New Web Generation*, JHEP **09** (2007) 028.

[28] A. Pukhov et al., *CompHEP: a package for evaluation of Feynman diagrams and integration over multiparticle phase space*, hep-ph/990828.

[29] E.Boos et al., *CompHEP 4.4: Automatic computations from Lagrangians to events*, Nucl. Instrum. Meth. **A 534** (2004) 250.

[30] ATLAS Collaboration, *Electron performance measurements with the ATLAS detector using the 2010 LHC proton-proton collision data*, arXiv:hep-ex/1110.3174.

[31] ATLAS Collaboration, *Performance of primary vertex reconstruction in proton-proton collisions at* $\sqrt{s} = 7$ *TeV in the ATLAS experiment*, ATLAS-CONF-2010-069.

[32] ATLAS Collaboration, *Muon reconstruction efficiency in reprocessed 2010 LHC proton-proton collision data recorded with the ATLAS detector*, ATLAS-CONF-2011-063.

[33] T. Junk, *Confidence level computation for combining searches with small statistics*, Nucl. Instr. Meth. A **434** (1999) 435.

[34] T. Junk, *Confidence Level Computation for Combining Searches with Small Statistics*, http://root.cern.ch/root/doc/TomJunk.pdf, hep-ex/9902006.